Proceedings of the ASME 2016 35th International Conference on Ocean, Offshore and Arctic Engineering
OMAE2016
June 19-24, 2016, Busan, South Korea

OMAE2016-54956

Motion-Based Wave Inference: Monitoring Campaign on a Turret FPSO

Iuri Baldaconi da Silva Bispo
Numerical Offshore Tank (TPN)
University of São Paulo
São Paulo,SP, Brazil

Asdrubal N. Queiroz Filho
Numerical Offshore Tank (TPN)
University of São Paulo
São Paulo,SP, Brazil

Eduardo A. Tannuri
Numerical Offshore Tank (TPN)
University of São Paulo
São Paulo,SP, Brazil

Alexandre N. Simos
Naval Arch & Ocean Eng. Dept.
University of São Paulo
São Paulo,SP, Brazil

ABSTRACT

In recent years, considerable effort has been made in order to validate different methods that aim at estimating the wave spectra from the motions recorded on a ship or on an offshore platform. For more than ten years now, the University of São Paulo has been working on a wave inference method for moored oceanic systems, such as Floating Production Storage and Offloading (FPSO) vessels.

This paper brings the first results from an ongoing field campaign, started in December 2014, for the estimation of wave statistics by means of this system, which is based on a Bayesian inference approach. The performance of the motion-based method is checked against the wave estimations provided by a commercial marine radar system. The radar is installed in a fixed platform close to the FPSO that is being monitored, which is moored in a turret configuration. Comparison between both systems allows one not only to evaluate the performance of the method but also to evaluate the inherent limitations that exist when the estimations are based on a very large vessel, especially one whose heading may be subjected to fast variations.

In this work, a new algorithm for the partition of the wave spectrum is used, differing from the previous works. This technique allows the identification and combination of energy peaks of the directional spectrum into wave systems, providing better modal wave statistics and less noise in the final spectrum.

Previously validation of the wave inference method was made through numerical and small-scale experimental analysis. Also, in previous studies, a 9-month field campaign was also used to validate the Bayesian method using a spread-moored FPSO, but no comparison to other measurement technique was made, instead, numerical forecasts were adopted. In this work this objective is achieved: so far, 10 months of estimates from the Bayesian inference algorithm have already been compared to data supplied by a radar system.

Comparisons with the marine radar readings attest an adequate identification of mean wave directions, with the Bayesian model estimating mean wave directions that are in close agreement to those provided by the radar system most of the time. There are, however, a few cases when the discrepancy is large and the reasons for this are still under investigation.

The comparison between both sources of data provides some insightful results, which are discussed in this paper. First, they confirm and quantify the main biases of the applied method, which are related to the filtering of the energy from high-frequency waves. On the other hand, they attest that the performance of the method for more severe sea states is good overall, showing that the method is able to provide good estimates of wave height and direction and also to capture situations when wave conditions are changing fast, such as the ones that occur with the incoming of cold fronts from South.

KEYWORDS

Wave spectra, Bayesian estimation, Turret-moored FPSO, marine radar, partitioning algorithm.

INTRODUCTION

A considerable effort has been made by several research groups during the last decade in order to produce good quality

wave estimation from the record of vessels' motions (see for example Iseki and Ohtsu [2], Nielsen [3] and Simos et al. [4])

When compared to other wave monitoring systems, such as buoys or marine radar systems, the main advantage that arises concerns the simplicity of the instrumentation (composed basically of accelerometers and rate-gyros), which is very easy to install on-board and, furthermore, requires a rather uncomplicated maintenance, especially if compared to the wave buoys. On the other hand, this method has obvious limitations: only waves that impose a reasonable level of motions to the vessel may be estimated. This is due to the fact that the vessel acts as a low-pass filter, filtering the energy contained in high frequency wave components that do not excite the vessel's first-order response.

Therefore, the performance of the method is expected to be good for waves of relatively high periods, including more severe sea states. By the limitation imposed on the frequency range, it is evident that, the larger the ship, the narrower this range will be: Large-displacement vessels, such as the Very Large Crude Carriers (VLCC) on which the FPSOs are usually based, will have lower cut-off frequencies when compared to smaller vessels, such as a crane-barge, for example. Consequently, when based on a FPSO, it is obviously not envisaged as a substitute for wave buoys for the sake of long-term oceanographic records. However, it may provide important information concerning the operation of such vessels when the problems are directly connected to the waves in the range of frequencies that do impose significant motions to the floating unit.

This paper addresses the preliminary results from an on-going field campaign for wave spectra estimation from the measurements of the first order motions of a turret-moored FPSO located offshore Brazil. It is a natural continuity of the research conducted at University of São Paulo and since the last works that were published on it, such as [11] and [12], some new functionalities of the wave estimation system were implemented.

Previous validations were based on small scale experiments ([3], [4], [6]) and in a 9-month real-scale campaign [11], and this present work introduces a new dataset of estimates, based on a different motion basis. Also, a new algorithm for the identification of multiple peaks of energy and the estimation of parameters for their combination into wave groups was implemented. The estimates obtained from this process are then compared to the dataset provided by a radar system installed in the vicinity to the FPSO, showing quite reasonable agreement.

An overview of the theory behind the so called Bayesian estimation method is presented in the next section. Following that, the algorithm adopted for identification and combination of peaks and the estimation of their statistical parameters is described. Sample results obtained from the 10-months data records are presented and compared to the radar estimates; a discussion is then made on the level of agreement observed between the data from the two different sources. Finally, some questions are posed in order to indicate the next steps of the research.

BAYESIAN ALGORITHM

A Bayesian inference method, which is detailed in this section, is used for the estimation of the wave spectra.

The main concept behind this method is that the errors between the estimated and the true spectra can be modeled as a Gaussian white noise and the minimization of these errors imply directly in the maximization of the probability that the estimated spectrum is the one which generated the measured motions of the ship.

This approach to solving the inverse problem defined by the wave spectrum that generated a particular measurable quantity was firstly introduced by Hashimoto and Kobune [1] and later adapted by Iseki and Ohtsu [2] for the use of recorded time series of motions of a vessel, using the (cross-) power spectra of this series.

Since those first studies, many improvements have been made to this method, such as the introduction of a second hyperparameter, presented in Nielsen [3], so that direction and frequency could be controlled in order to find a smoother or a noisier solution. Also in Bispo et al. [8], the range of values of the hyperparameter related to direction is predefined as a function of the mean period of heave (T_z), which is strongly correlated to the peak period of the waves, the variable of dependency of the hyperparameter.

The algorithm is basically defined by the maximization of the product between the likelihood function and a prior distribution, in which the former is the probabilistic representation of the error between the estimated and the true spectrum, and the latter represents the previous information regarding the unknown coefficients (properties such as smoothness of the directional wave spectrum, in our case). This principle is based on Bayes' theorem and it is applied in order to provide a useful mathematical algorithm for the motion-based wave estimation. The theory related to this method is well documented in literature and therefore will not be addressed here (See [9] or [13], for example).

In previous works, such as in Simos et al. ([4], [6] and [11]), Tannuri et al. [7] and Bispo et al. [8], only the roll motion is not considered in the basis used for the estimation process, due to nonlinearities in its transfer function. In the present work, a new base of motions is employed instead, composed by sway, heave and pitch motions. The yaw motion was discarded because of reading errors.

A basic assumption is that the relation between waves and ship response is linear and therefore, the cross-spectra derived from the time series of ship motions (ϕ_{ij}) and the directional wave spectrum can be related to the RAOs through the following integral:

$$\phi_{ij}(\omega) = \int_{-\pi}^{\pi} RAO_i(\omega,\theta).RAO_j^*(\omega,\theta).S(\omega,\theta).d\theta \qquad (1)$$

where RAO_i denotes the Response Amplitude Operator of the motion $i = \{1,2,3,4,6\}$ at frequency ω and direction of incidence θ and $S(\omega, \theta)$ denotes the directional wave spectrum.

The discrete expression of (1) is derived assuming the integrand to be constant on each slice $\Delta\theta = 2\pi/K$, where K is the number of steps for discretization in θ,

$$\phi_{ij}(\omega) = \Delta\theta \sum_{k=1}^{K} RAO_i(\omega, \theta_k).RAO_j^*(\omega, \theta_k).S(\omega, \theta_k).d\theta \quad (2)$$

with $\theta_k = -\pi + (k-1)\Delta\theta$.

A certain range of M wave frequencies is specified in advance $(\omega_1, \omega_2, \dots, \omega_m, \dots, \omega_M)$ and, in this study, discretization is refined in most relevant frequencies.

By assuming that measurement errors occur, Eq.(2) can be written in matrix notation as in Eq.(3), from the total of (N) measured vessel's motions $\phi_{ij}(\omega_m)$:

$$\mathbf{B} = \mathbf{A}.\mathbf{x} + \mathbf{U} \quad (3)$$

Where:

B is the vector of $(N^2 \cdot M)$ elements related to the spectrum and cross-spectrum and is given by:

$$\mathbf{B} = \begin{bmatrix} \mathbf{b_1} \\ \mathbf{b_2} \\ \vdots \\ \mathbf{b_M} \end{bmatrix}, \qquad \text{with } \mathbf{b}_m = \begin{bmatrix} \boldsymbol{\phi}_{ii}(\boldsymbol{\omega}_m) \\ \vdots \\ \mathbf{Re}[\boldsymbol{\phi}_{ij}(\boldsymbol{\omega}_m)] \\ \vdots \\ \mathbf{Im}[\boldsymbol{\phi}_{ij}(\boldsymbol{\omega}_m)] \\ \vdots \end{bmatrix} \quad (4)$$

A is a $(N^2 \cdot M) \times (K \cdot M)$ matrix, representing the transfer functions of the employed d.o.f. (RAOs):

$$\mathbf{A} = \begin{bmatrix} \mathbf{A}_1 & \mathbf{0} & \mathbf{0} & \cdots & \mathbf{0} & \mathbf{0} \\ \mathbf{0} & \mathbf{A}_2 & \mathbf{0} & \cdots & \mathbf{0} & \mathbf{0} \\ \mathbf{0} & \mathbf{0} & \ddots & \mathbf{0} & \mathbf{0} & \mathbf{0} \\ \vdots & \vdots & \mathbf{0} & \mathbf{A}_m & \mathbf{0} & \mathbf{0} \\ \mathbf{0} & \mathbf{0} & \mathbf{0} & \mathbf{0} & \ddots & \vdots \\ \mathbf{0} & \mathbf{0} & \mathbf{0} & \mathbf{0} & \cdots & \mathbf{A}_M \end{bmatrix} \quad (5)$$

where $\mathbf{0}$ is the $(N^2 \times K)$ matrix with null elements and $\mathbf{A}_m$ is the RAO matrix:

$$\mathbf{A}_m = \begin{bmatrix} |RAO_i(\omega_m,\theta_1)|^2 & \cdots & |RAO_i(\omega_m,\theta_k)|^2 & \cdots & |RAO_i(\omega_m,\theta_K)|^2 \\ \vdots & & \vdots & & \vdots \\ \mathbf{Re}[RAO_i(\omega_m,\theta_1)RAO_j^*(\omega_m,\theta_1)] & \cdots & \mathbf{Re}[RAO_i(\omega_m,\theta_k)RAO_j^*(\omega_m,\theta_k)] & \cdots & \mathbf{Re}[RAO_i(\omega_m,\theta_K)RAO_j^*(\omega_m,\theta_K)] \\ \vdots & & \vdots & & \vdots \\ \mathbf{Im}[RAO_i(\omega_m,\theta_1)RAO_j^*(\omega_m,\theta_1)] & \cdots & \mathbf{Im}[RAO_i(\omega_m,\theta_k)RAO_j^*(\omega_m,\theta_k)] & \cdots & \mathbf{Im}[RAO_i(\omega_m,\theta_K)RAO_j^*(\omega_m,\theta_K)] \\ \vdots & & \vdots & & \vdots \end{bmatrix}$$

U is a $(N^2 \cdot M)$ vector of measurement errors included in order to facilitate the Bayesian modeling (see [9] for details) and it is assumed to be a Gaussian white noise sequence with zero mean and variance σ^2.

The vector **x** contains the unknown elements of the spectrum, evaluated at the $(K \cdot M)$ pairs (ω_m, θ_k):

$$\mathbf{x} = \begin{bmatrix} S(\omega_1,\theta_1) \\ S(\omega_1,\theta_2) \\ \vdots \\ S(\omega_M,\theta_{K-1}) \\ S(\omega_M,\theta_K) \end{bmatrix} \quad (6)$$

The Bayesian procedure is then applied to the system in Eq.(3), and by doing this, the unknown coefficients in Eq.(6) can be estimated by maximizing the product of the likelihood function by the prior distribution. The likelihood function is the conditional probability of occurrence of a given measurement (Eq. (4)), given the directional spectrum (Eq. (6)). Since measurement noise is assumed to be Gaussian, it can be shown (see [2]) that the likelihood function $L(\mathbf{x}|\mathbf{B})$ is given by:

$$L(\mathbf{x}|\mathbf{B}) = \left(\frac{1}{2\pi\sigma^2}\right)^{N^2/2} \exp\left(-\frac{1}{2\sigma^2}\|\mathbf{B} - \mathbf{A}\mathbf{x}\|^2\right) \quad (7)$$

The previous information about the wave spectrum, represented as unknown coefficients in **x,** is given by the assumption that the spectrum is smooth in both direction and frequency. This is represented in the Bayesian approach as the prior distribution as follows.

Second order differences are defined by the expressions below (8). The first, $\varepsilon_{1_{mk}}$, is associated to direction k at frequency m and the second, $\varepsilon_{2_{mk}}$, associated to the frequency m at the direction k:

$$\begin{aligned} \varepsilon_{1_{mk}} &= S(\omega_m,\theta_{k-1}) - 2S(\omega_m,\theta_k) + S(\omega_m,\theta_{k+1}), \\ \varepsilon_{2_{mk}} &= S(\omega_{m-1},\theta_k) - 2S(\omega_m,\theta_k) + S(\omega_{m+1},\theta_k) \end{aligned} \quad (8)$$

By keeping the summations in Eqs.(9) and (10) as small as possible, the smoothness assumption should be satisfied. In this fashion, the prior distributions are mathematically expressed in terms of the unknown coefficients that describe the wave spectrum:

$$\sum_{k=1}^{K}\sum_{m=1}^{M} {\varepsilon_{1_{mk}}}^2 = \mathbf{x}^T\mathbf{H}_1\mathbf{x} \quad (9)$$

with $S(\omega_m,\theta_0) = S(\omega_m,\theta_K)$ and $S(\omega_m,\theta_{K+1}) = S(\omega_m,\theta_1)$, and

$$\sum_{k=1}^{K}\sum_{m=1}^{M} {\varepsilon_{2_{mk}}}^2 = \mathbf{x}^T\mathbf{H}_2\mathbf{x} \quad (10)$$

where the matrixes $\mathbf{H}_1$ and $\mathbf{H}_2$ may be easily constructed considering the proper definition of the vector **x** (see, for example [7]).

Since the vessel does not provide a significant response for some wave frequencies, any amount of energy could be estimated within this range. To avoid this issue on the estimation of the wave spectrum, the sum of the power of the spectrum is minimized in a pre-defined range of low and high frequencies given by $(\omega_1, \omega_2, \dots, \omega_L, \omega_H, \dots, \omega_M)$. This is mathematically described by the introduction of a third

constraint to the problem, providing the minimization of the following functional (matrix $\mathbf{H_3}$ is obtained by a procedure similar to the one used to derive $\mathbf{H_1}$ and $\mathbf{H_2}$):

$$\sum_{k=1}^{K}\sum_{m=1}^{L} S(\omega_m,\theta_k)^2 + \sum_{k=1}^{K}\sum_{m=H}^{M} S(\omega_m,\theta_k)^2 = \mathbf{x}^T\mathbf{H}_3\mathbf{x} \qquad (11)$$

Considering that each of these prior distributions is defined based on Gaussian variables, with zero mean and variances σ^2/u_1^2; σ^2/u_2^2 and σ^2/u_3^2 for distributions (9), (10) and (11), respectively, the product of the likelihood function (7) by the overall prior distribution $p(\mathrm{x})$ is given by:

$$L(\mathbf{x}|\mathbf{B}).\,p(\mathbf{x}) = C.\exp\left\{-\tfrac{1}{2\sigma^2}\left[\|\mathbf{B}-\mathbf{A}\mathbf{x}\|^2 + \mathbf{x}^T(u_1^2\mathbf{H}_1 + u_2^2\mathbf{H}_2 + u_3^2\mathbf{H}_3)\mathbf{x}\right]\right\} \qquad (12)$$

with C being a scale factor independent of the model variable **x**.

The hyperparameters u_1 and u_2 operate in order to preset the level of smoothness desired in direction and frequency, respectively, since the minimization of Eqs. (9) and (10) imply in the reduction of noise. These two hyperparameters are chosen based on considerations presented in [8], including the variation of $u_1$as function of T_z of heave.

Minimize the functional $J(\mathbf{x})$ given by Eq.(13) below through a quadratic programming algorithm is also to maximize Eq.(12), which is, in turn, to find the most probable spectrum that generated the measured motions.

$$J(\mathbf{x}) = \|\mathbf{B}-\mathbf{A}\mathbf{x}\|^2 + \mathbf{x}^T(u_1^2\mathbf{H}_1 + u_2^2\mathbf{H}_2 + u_3^2\mathbf{H}_3)\mathbf{x} \qquad (13)$$

This problem has $(\mathrm{K}\cdot\mathrm{M})$ variables, since the number of directions is (K) and the number of frequencies is (M).

The vector **x** that minimizes Eq. (13) is the output of the Bayesian algorithm and it is thereafter rearranged into a matrix that represents the energy spectrum, dependent on wave periods and directions.

WAVE STATISTICS

Considering the matrix representation of $S(\omega,\theta)$ and the corresponding spectral moment m_n of the wave spectra given by:

$$m_n = \int_0^{2\pi}\int_0^{\infty} \omega^n.S(\omega,\theta)\,d\omega d\theta \qquad (19)$$

The non-directional sea state parameters, significant height and mean wave period, are respectively derived by Eqs. (20) and (21) below:

$$H_s = 4.\sqrt{m_0} \qquad (20)$$

$$T_{01} = 2\pi\frac{m_0}{m_1} \qquad (21)$$

As for the mean direction, θ_m, which describes the average distribution of the energy contained in the spectrum, the calculation is performed according to the following expression:

$$\theta_m = \arctan\left(\frac{\overline{\sin\theta}}{\overline{\cos\theta}}\right) \qquad (22)$$

where:

$$\overline{\sin\theta} = \frac{\iint \sin\theta S(\omega,\theta)d\omega d\theta}{\iint S(\omega,\theta)d\omega d\theta}$$

and

$$\overline{\cos\theta} = \frac{\iint \cos\theta S(\omega,\theta)d\omega d\theta}{\iint S(\omega,\theta)d\omega d\theta}$$

Expressions (20) to (22) provide the sea wave statistics that are used for comparison to the ones given by the radar system, which are also obtained by these same expressions, but with calculations performed by the manufacturer's software.

PARTITIONING SCHEME

Although the mentioned global statistics, H_s, T_{01} and θ_m, are used to compare the general performance of the estimation method presented in this study, the spectra can be compared in detail by observing the statistics for *wave systems* identified in each estimated directional spectrum. Also, using a partitioning scheme, the filtering of low energy peaks is performed more efficiently, leading to a more consistent comparison of the statistics provided by the radar. A representation of the partitioning of a spectrum is given in Figure 1 below:

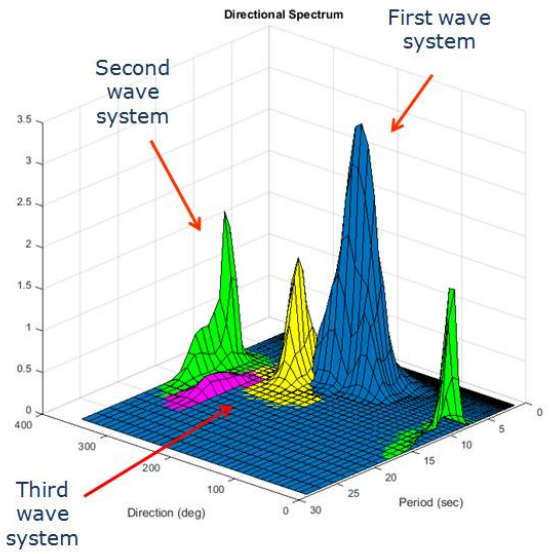

Figure 1: Illustrative representation of a spectrum, depicting distinct wave systems: the nature of generation for each one can be from a different source and, therefore, the characteristics represented by each group statistics can vary greatly in direction and peak period.

In order to investigate each peak individually, the complete spectrum must be partitioned in different spectra in a

process that can identify adjacent peaks as belonging to the same wave system. In a previous implementation of the algorithm, presented in Tannuri et al. [11], only peak identification was considered, so that no combination or grouping was performed. In that, residual noise could be interpreted as valid energy peaks, distorting the global statistics as well.

The process of extracting the statistics that describe each energy group identified in the directional wave spectrum is based on the spectral partitioning algorithm presented by Hanson and Phillips [10] and it is briefly described in this section. The relationship $S(f,\theta) = 2\pi S(\omega,\theta)$ is used to represent the spectra as function of frequency f in (Hz), which is used in this section to present the original formulation of spectral partitioning.

A quite straightforward method is applied to identify each energy peak in the matrix obtained by the Bayesian algorithm: it consists on finding paths of steepest ascent for each element of the matrix, taking into account the largest of the its six neighbors, leading to a final element where there is no larger neighbor, being the latter the maximum energy value of a peak.

This iterative process provides a matrix of largest neighbors for each element of the discrete spectrum. Based on this new matrix, a path of largest slope for each point in the original matrix can be established and an energy peak of the spectrum is defined as being the set of elements for which the path ends at the same matrix element. In other words: all points having a path that ends at the same largest energy value are considered to belong to the same energy peak.

Figure 2 below shows an energy peak with three of its points and their respective paths of largest slope. In conjunction with other elements of the spectral matrix, these form an energy peak.

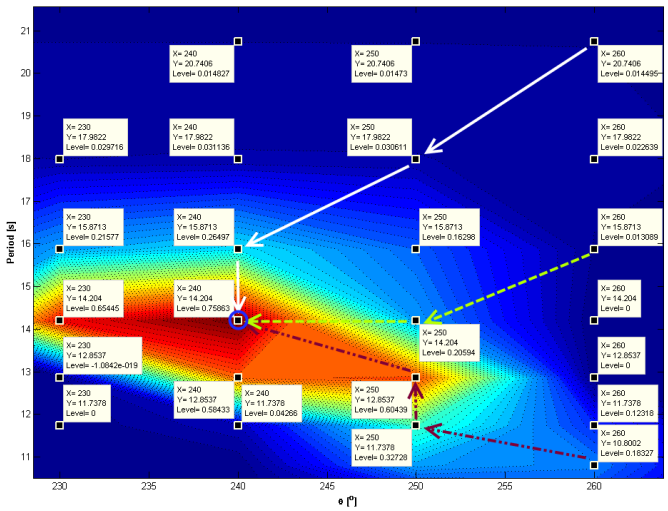

Figure 2: Schematic representation of the path finding algorithm.

Assuming that k-th identified energy peak can be represented as an unimodal directional spectrum, $S_k(f,\theta)$, the next step is to compute, for each identified partition, the total energy $e_k = \int_0^{2\pi}\int_0^{\infty} S_k(f,\theta)\, df d\theta$, the peak frequency f_p, the peak direction θ_p, and the peak energy $S_k(f_p,\theta_p)$ are computed.

The next step is to identify and remove from the main spectrum any partition in which the significant height, $H_{s_k} = 4.\sqrt{e_k}$, is below a threshold of 0.2 m. This values was established based on the observation of residual noise in the estimated spectra dataset and it was used to improve computational efficiency.

Following the original algorithm proposed in [10], wind sea peaks are identified and combined using a wave age criterion. Any energy partition whose maximum value, $S_k(f_p,\theta_p)$, lies within the parabolic region defined by expression (23) is considered to be generated by the wind and it is, therefore, combined with other peaks that may fall in to the same region. In this expression, U_{10} is the wind velocity measured at 10 m above the water level and β is the difference between wave and wind directions ($0 \leq \beta \leq \pi/2$).

$$f_p \geq \frac{g}{2\pi}(1.5\, U_{10}\, cos\, \beta)^{-1} \qquad (23)$$

After the wind sea partitions were identified, they are considered to belong to the same wave system, and are removed from the spectral matrix, which now holds only swell partitions.

Next, the remaining swell peaks are combined into the same wave system if, for any two adjacent peaks, at least one of the following rules holds true:

- Peak separation: Compare the distance between peaks Δf^2 with the spread of each individual peak, $\overline{\delta f^2}$. Peaks are combined into a wave system if $\Delta f^2 \leq \kappa\, \overline{\delta f^2}$, where κ is called spread factor.
- Valley criterion: If the lowest point between them is greater than the peak minimum factor, ζ, times the smallest of the two peak energies $S_k(f_p,\theta_p)$.
- If the peak energies, $S_k(f_p,\theta_p)$, for both are just one grid point apart.

Both κ and ζ are defined by optimization, as recommended by [10], based on the specific dataset in which the estimation is taking place, in order to reduce noise in the final spectrum. The values $\kappa = 0.4$ and $\zeta = 0.65$ were adopted after some tests.

The distance between peaks is computed, for adjacent peaks i and j, by:

$\Delta f^2 = \left(f_{px,i} - f_{px,j}\right)^2 + \left(f_{py,i} - f_{py,j}\right)^2$, where

$f_{px} = f_p \cos\theta_p$ and $f_{py} = f_p \sin\theta_p$.

And spread of each peak is given by:

$\overline{\delta f^2} = \overline{f_x^2} - \overline{f_x}^2 + \overline{f_y^2} - \overline{f_y}^2$, where

$$\overline{f_x} = \frac{1}{e_k}\int_f \int_\theta S_k(f,\theta) f \cos\theta \, \partial\theta \, \partial f,$$

$$\overline{f_y} = \frac{1}{e_k}\int_f \int_\theta S_k(f,\theta) f \sin\theta \, \partial\theta \, \partial f,$$

$$\overline{f_x^2} = \frac{1}{e_k}\int_f \int_\theta S_k(f,\theta) f^2 \cos^2\theta \, \partial\theta \, \partial f \quad \text{and}$$

$$\overline{f_y^2} = \frac{1}{e_k}\int_f \int_\theta S_k(f,\theta) f^2 \sin^2\theta \, \partial\theta \, \partial f.$$

The new partitions found by combination of the previous ones are also eligible for combination, so the process must be performed from the beginning every time a new partition is formed. After the combination of swell peaks into wave systems, an energy threshold check is performed in order to exclude noise in low energy regions. Any partition in which $e_k \leq \frac{A}{f_p + B}$, must be excluded from the spectral matrix. Parameters A and B are optimized to eliminate noise in low energy regions of the spectrum.

In this work, numerical integration is performed for all the above integrals using **trapz** function from MATLAB® 8.4.0.

FIELD CAMPAIGN ASPECTS

A monitoring campaign is currently underway in order to validate the wave estimation system and to test new features, and records already include data comprising a period of 10 consecutive months.

FPSO

This campaign is based on a turret-moored FPSO, located offshore Brazil, and started December/2014. The main dimensions of the FPSO are given in Table 1 and its location is presented in Figure 3 below:

Table 1 VLCC-FPSO main properties

Loading Condition	**Full**	**Interm.**	**Ballast**
Length Overall Lpp (m)	333.0		
Beam B (m)	58.0		
Draft T (m)	21.5	15.5	7.5
Displacement (ton)	3,19e+05	2,24e+05	1,04e+05
Rxx/B (%)	36,12	38,55	38,55
Ryy/Lpp (%)	22,87	24,08	26,94

Figure 3: Approximated location of the FPSO - Around 85 km from the shore and about 120 m depth. (Source: Google Earth)

Among the data received from the vessel, there is also the information about its draft, which is used to select the corresponding RAOs. These RAOs are stored in a pre-calculated database and were obtained using WAMIT® 7.0 for several loading conditions corresponding to a 0.5 m variation in draft. These transfer functions were calculated at steps of 10 degrees, from 0 to 180 degrees. The wave period discretization was made with a 0.25s step, between 4s and 20s, and with 1s between 20s and 30s.

Any needed value from the estimation algorithm is obtained by linear interpolation in these discretized ranges. In order to avoid spurious energy outside the range of frequencies with hull response, the following limits were adopted: $\omega_L = 0.21$rad/s and $\omega_H = 0.79$rad/s (values in real-scale, equivalent to wave periods of 30s and 8s, respectively). More details on the choice of these limits can be found in [12]. In this work, the order of the system defined in the Bayesian algorithm is (K.M), with K=36 (10^o intervals with respect to wave direction) and M=20.

The motion of the vessel is measured by an IMU, and the results are shown in an user interface very similar to the one presented in previous works, such as in [11] and [12], but with a few improvements (Figure 4).

The wave spectrum estimation system uses a record of motions of 30 minutes, with a sampling frequency of 1 Hz.

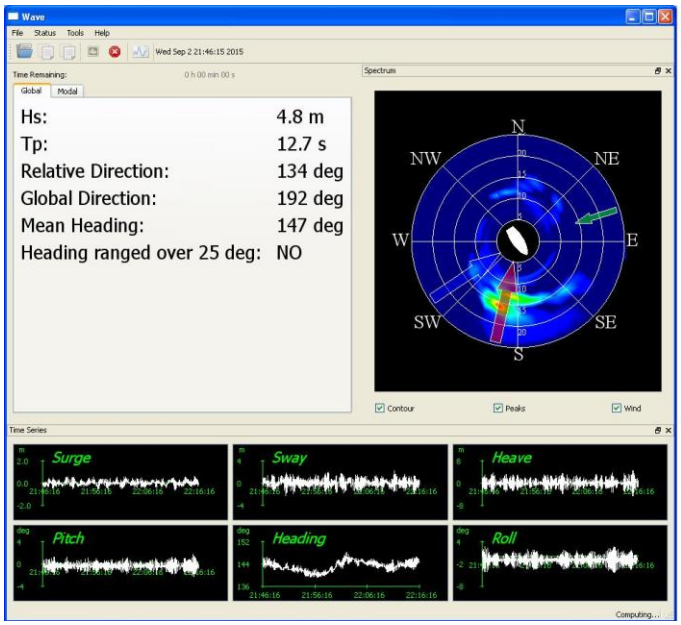

Figure 4: Wave estimation software – user interface

MARINE RADAR

The global wave statistics obtained from the Bayesian algorithm were compared to the respective ones provided by a commercial marine radar. This equipment is installed in a fixed platform located nearby the FPSO (approximately 7 km), so that the estimates used for comparison do not have significant influence from the distance.

Estimates provided by the radar system can be accessed in two ways: sea wave statistics or directional wave spectrum files, each one containing this data at 2 minutes intervals for a whole day. The first kind of file gives global and modal statistics for two energy peaks. As for the spectrum file, it can be used in the same way that the matrix obtained from the Bayesian algorithm: going through the process of partitioning the spectrum and extracting the global and modal statistics.

Since the main output is composed by the series of global statistics, which are, in turn, the most usual data used for comparison in this field of research, the first files are adopted for comparison to the respective global statistics obtained by the Bayesian method, so that no biases are introduced in the data by the partitioning algorithm.

In the comparison of the spectra, the global statistics are also used, but since the modal statistics can describe the spectrum in much more detail, these were adopted and extracted from both sources using the partitioning algorithm.

ESTIMATED DATA COMPARISON

GLOBAL WAVE STATISTICS

In this section, the global statistics of the directional wave spectra obtained from the Bayesian algorithm are compared to the ones provided by the radar system.

It was noted from previous works ([4]-[7], [11] and [12]) that the response from VLCC are quite attenuated for wave periods smaller than 8s. This fact implies that the estimation method output is not reliable for such range of wave periods.

Regarding the mean direction, values are given with respect to the earth-fixed system: zero degrees indicating waves coming from North, 90 degrees coming from East and so on.

The data were divided into periods of approximately 30 days and some illustrative results are presented in the following. The first period corresponds to the month of December, so during the summer season when waves conditions are generally mild. In this situation, mean periods are typically low and many times a significant part of the energy is outside the range of the motion-based estimations.

In spite of that, it can be seen that for significant wave heights higher than 1m (Figure 5) there is a reasonable agreement between the data sources, especially when the mean wave period is larger than 8s, as presented in Figure 6.

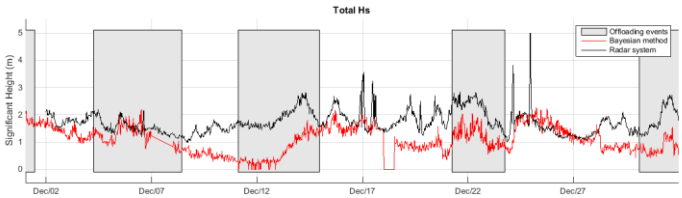

Figure 5: Global significant wave height - Bayesian vs Radar - December/14.

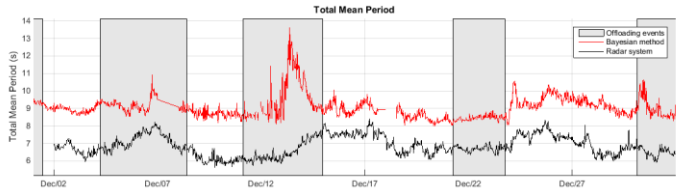

Figure 6: Global mean wave period - Bayesian vs Radar - December/14.

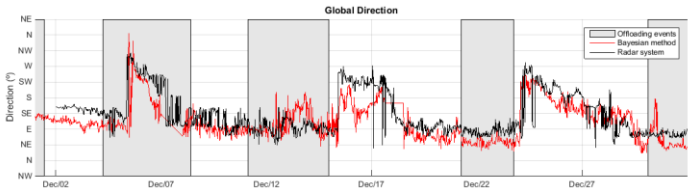

Figure 7: Global mean direction - Bayesian vs Radar - December/14.

As mentioned before, this tendency of better estimations when there is a larger mean period is related to the fact that the ship acts as a filter of high frequency waves, so that only the low period part of the wave spectra is properly estimated. This is clearly shown in Figure 6, where the estimated values of mean period are bounded in 8s.

It should be noticed, however, that despite the natural filtering of part of the energy, there is a fairly good in the mean wave directions measured by both methods, as presented in Figure 7.

Another important feature must be stressed in this case. During the month of December there were three events associated to the passage of cold-fronts that are clearly registered by both methods. During these events, wave direction typically changes from NE (the prevailing wave direction in the region) to SW in a short period of time, following the change in the mean wind direction. This explains the rapid changes observed in Figure 7. Also, during summer season these events are generally mild so they do not increase the wave height significantly.

The grey blocks presented in the figures above indicate periods when an offloading operation was taking place. These events are being monitored for observing whether they may compromise the data due to the presence of the shuttle tanker. Analysis of data recorded so far indicates that the offloading operations did not have a significant interference with the process of estimation.

It can be observed, by the series presented in Figure 8, that the significant wave height was higher during the South-Hemisphere winter-spring (W-S) period when compared to the summer season (Figure 5).

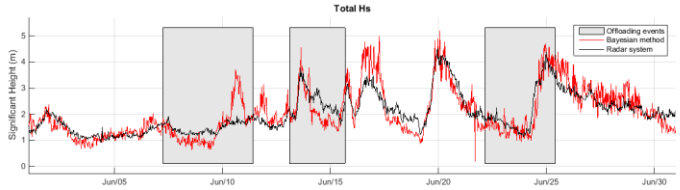

Figure 8: Global significant wave height - Bayesian vs Radar - June/15.

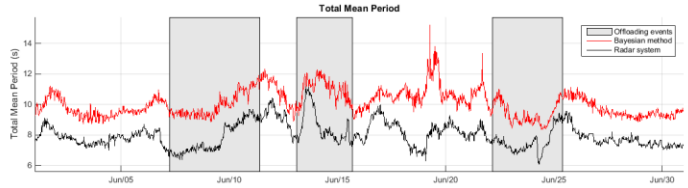

Figure 9: Global mean wave period - Bayesian vs Radar - June/15.

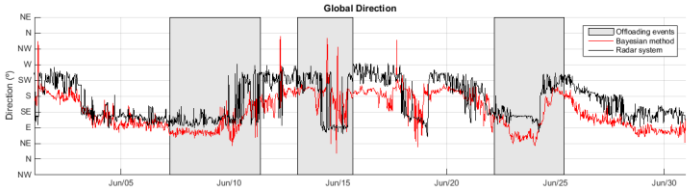

Figure 10: Global mean direction - Bayesian vs Radar - June/15.

Also the estimates of T_{01} are larger for this period, as indicated by the radar estimates in Figure 9. Again, many storms associated to cold-fronts passed by during the month of June, as may be inferred from the changes in the mean wave direction (Figure 10). In these cases, however, mean wind speeds are high enough in order to produce significant growths in the significant wave heights, that in this case reached values close to 5m (Figure 5). Both methods now agree very well in the predictions of both wave height and directions, since wave conditions were within the range of estimations of the motion-based method for the whole period.

Next, an analysis of the correlation of records is presented. Periods of consecutive 30-days were selected and had their correlations between global H_s and θ_m from both data sources computed, being presented in Table 2.

The limitation provided by the estimates of T_{01}, which is bounded at 8s, leads to poor values of correlation between the estimates given by the radar system and the ones from the Bayesian method. Since the estimates of this parameter have information from distinct areas of the wave spectra, values from both sources at the same instant of time tend to be not correlated. Therefore, in order to have a fair comparison, the correlations of H_s and θ_m presented in Table 2 are computed disregarding points of the time series in which T_{01} is smaller than 8s.

Table 2: Correlation between series of H_s and θ_m

Period	H_s	θ_m
12/02/2014 to 01/02/2015	0.27	0.80
01/02/2015 to 02/02/2015	0.32	0.65
02/02/2015 to 03/06/2015	0.46	0.54
03/06/2015 to 04/06/2015	0.63	0.45
04/06/2015 to 05/08/2015	0.71	0.60
05/08/2015 to 06/09/2015	0.78	0.81
06/09/2015 to 07/19/2015	0.75	0.79

From these results, it can be seen that from March to August there is a better agreement for H_s. This illustrates the fact that during Winter-Spring period, the waves have larger periods and significant heights and, therefore, the motion of the ship improves, providing better information to the Bayesian algorithm. This also improves the estimation of θ_m, as it is shown by the correlations from June to August, although the mean direction is clearly less affected by the filtering of energy.

The correlation between these two data sources can be evaluated graphically in a scatter plot for H_s. As presented in Figure 11 to Figure 13, it is quite evident that from summer to winter the overall agreement between the two data sets improves drastically.

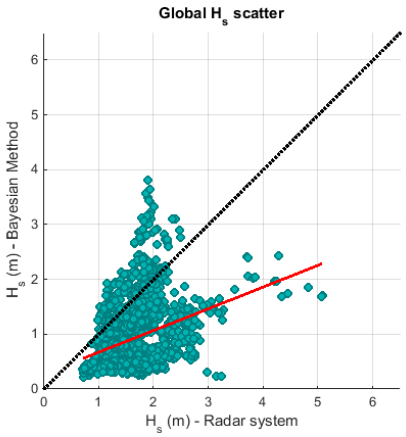

Figure 11 Global significant height comparison - Bayesian vs Radar - January/2015.

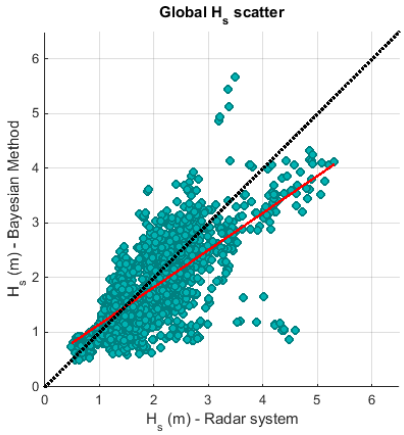

Figure 12 Global significant height comparison - Bayesian vs Radar - April/2015.

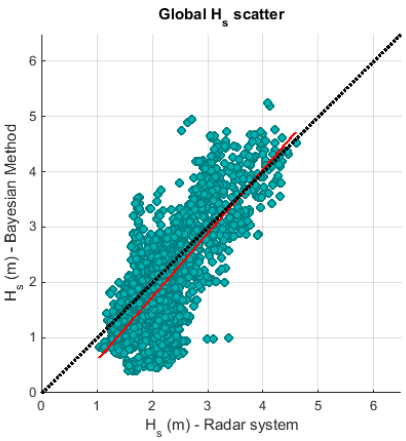

Figure 13 Global significant height comparison - Bayesian vs Radar - July/2015.

ENERGY SPECTRA

Although the overall performance of the method shows some promising results, a closer look must be taken into the estimated wave spectra, since series of global tendencies do not provide an insight on how the energy is distributed around the ship.

Two estimates of the directional wave spectrum were selected to illustrate distinct cases of estimation. The first one, relative to the time series from the half hour prior to 03/23/2015 19:47, has its statistics presented in Figure 14. The estimated spectra are presented in Figure 15 and Figure 16.

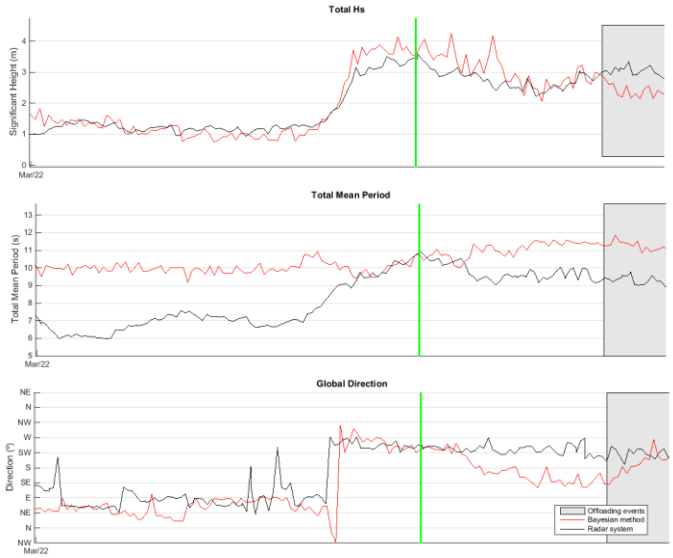

Figure 14: Series of statistics closer to 03/23/2015 19:47 - An example of a very good estimation of the wave spectrum and, therefore, of the wave main parameters.

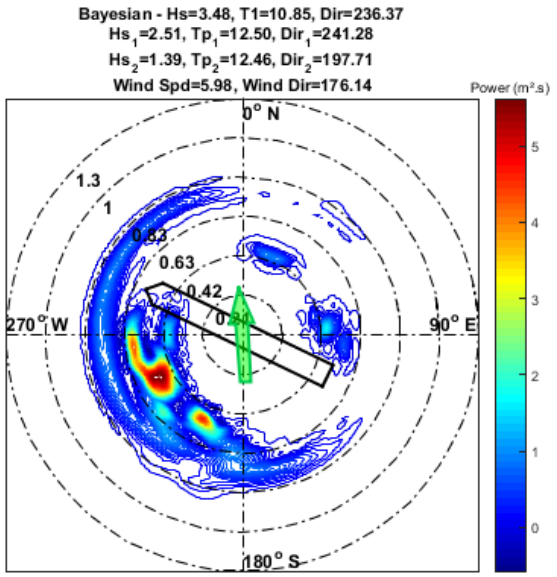

Figure 15: Directional wave spectrum obtained by the Bayesian method for the case of 03/23/2015 19:47.

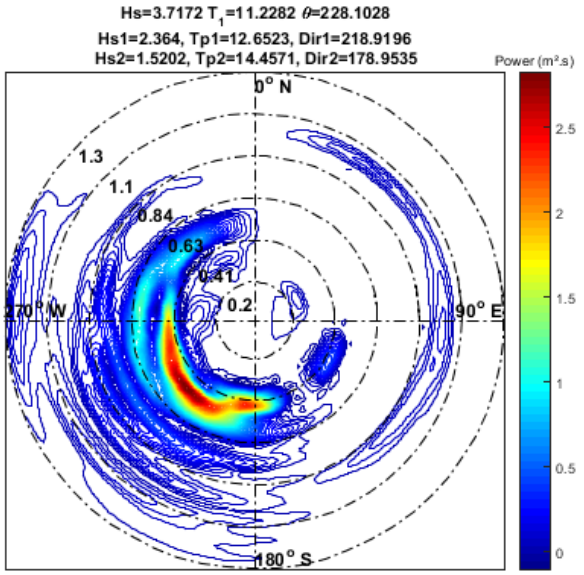

Figure 16: Directional wave spectrum obtained by the radar system for the case of 03/23/2015 19:47.

This case shows a very good estimation of the directional wave spectra, in which not only the global statistics from the Bayesian method and from the radar are close, but also the directional spectra have a very similar energy distribution. This fact is confirmed by the modal statistics, which are quite close from each other. Also, in Figure 14, is possible to see that this tendency holds for a while, being quite stable.

The second case is related to the half hour series of motions prior to 05/13/2015 15:13. In this case, for a short period of time, there is an overestimation of the H_s provided by the Bayesian method. In Figure 17 is possible to see that the total significant height is estimated as almost 6m, which is quite high for the Brazilian coast.

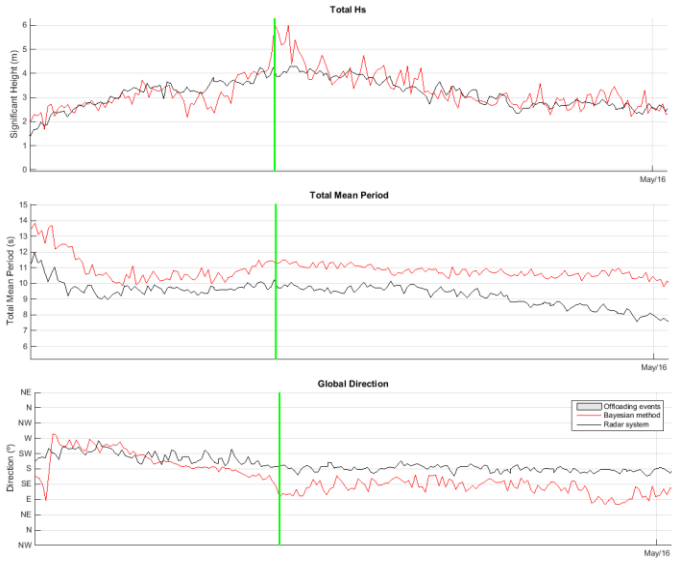

Figure 17: Series of statistics closer to 05/13/2015 15:13 - An example of an overestimated wave spectrum.

Estimates given by the radar system indicate that $H_s = 4$ m in that time period. During this overestimation of the energy, there is a tendency of a spurious energy peak to be estimated by the Bayesian method closer to bow of the vessel, when in fact the wave is coming closer to the beam direction.

The respective spectra for the Bayesian method and the radar system are presented in Figure 18 and Figure 19, where this sort of incorrect estimation can be clearly seen, specially for the mean direction estimate.

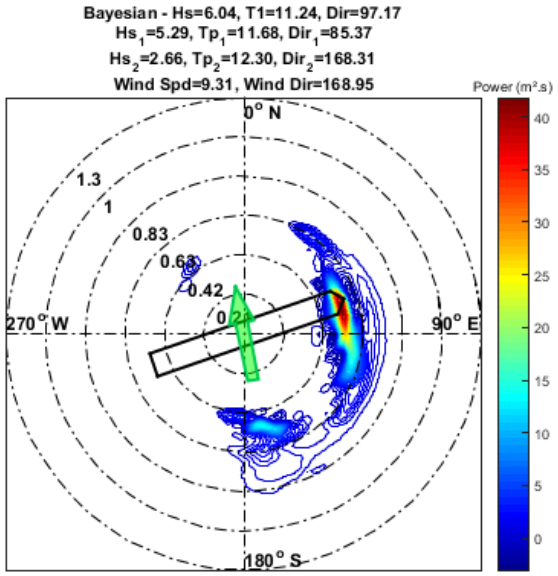

Figure 18: Directional wave spectrum obtained by the Bayesian method for the case of 05/13/2015 15:13.

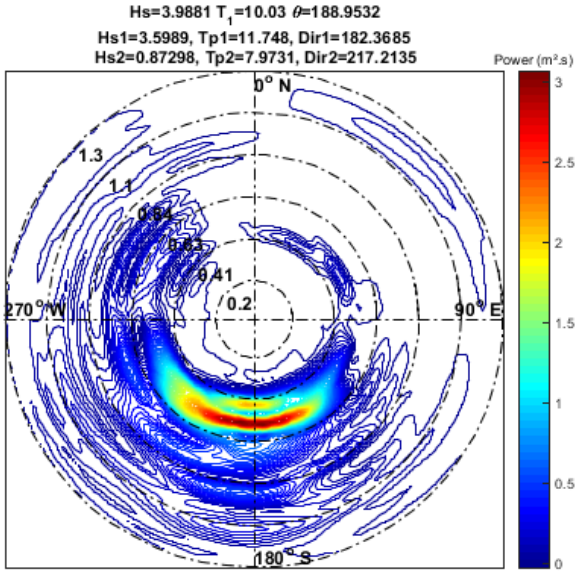

Figure 19: Directional wave spectrum obtained by the radar system for the case of 05/13/2015 15:13.

This sort of problem is infrequent, but it was observed in other occasions. It may be related to measurement errors or to

some sort of discrepancy in the numerical model of the vessel. The reasons for this kind of discrepancy are still under investigation.

CONCLUSIONS

The field campaign, started in December 2014 and yet in course, is providing some insightful results so far, confirming some observed tendencies from previous works.

Comparison for results indicates good correlation, in terms of the fluctuations in time, mainly for H_s and $\theta_m$during periods of time when the sea state is rough (as it gets towards winter). Estimates for H_s clearly show that the performance of the method improves from summer to winter, as expected, since the wave heights are higher (and so is the mean period) and the incoming cold fronts from South are more frequent. For mild seas, however, the estimates of this wave parameter show reasonable agreement for cases where $T_{01}$is greater than 8s and poor correlation to the wave radar results otherwise. These results contribute to the validation of this implementation of the Bayesian method based on the motions of the vessel.

The results are also confirming and quantifying some previous indications of biases, since it is known that the main limitation of the motion-based Bayesian method implemented for a VLCC concerns the filtering of high frequency wave components by the vessel. This leads to a bias: underestimation of the wave height and, on the other hand, overestimation of the mean wave periods. These trends tend to be more intense for mild sea conditions, as those that prevail through the summer season in the Brazilian shore and, through the collected data, it is possible to observe them.

Moreover, the comparisons with the measurements from the marine radar attest an adequate identification of mean wave directions: Bayesian model estimates mean wave directions that are in close agreement to those estimated by the radar system most of the time. There are, however, infrequent events when the discrepancy is large and the reasons for this are under investigation.

The good agreement in direction estimates is mainly stated by the resolution in time: is possible to observe the changes from the prevailing direction, East, to the South or South-West, when there is an incoming cold front from South, a very characteristic seasonal occurrence for the Brazilian coast.

ACKNOWLEDGMENTS

Authors are indebted to Statoil Brasil Óleo e Gás Ltda for supporting the research and for making the field campaign possible. Authors also wish to thank Petrobras for authorizing the use of the motion-based wave inference package in this research project. Eduardo Aoun Tannuri and Alexandre Nicolaos Simos acknowledge the Brazilian Research Council (CNPq) for their respective research grants. Iuri Baldaconi da Silva Bispo also would like to thank the Institute for Technological Research (IPT) for the granted license time, which was dedicated to this research.

REFERENCES

[1] Hashimoto, N.; Kobune, K, 1988. "Directional spectrum estimation from a Bayesian approach". Coastal Engineering Proceedings, pp.62–76.

[2] Iseki, T., and Ohtsu, K., 2000, "Bayesian estimation of directional wave spectra based on ship motions", Control Engineering Practice, 8, pp.215-219.

[3] Nielsen, U.D., 2008, "Introducing two hyperparameters in Bayesian estimation of wave spectra". Probabilistic Engineering Mechanics, 23, pp. 84-94.

[4] Simos A.N., Tannuri, E.A., Sparano, J.V., Matos, V.L.F., 2010, "Estimating wave spectra from the motions of moored vessels: Experimental validation". Applied Ocean Research 32, pp.191-208.

[5] Tannuri, E. A., Simos, A.N., Sparano, J.V., Cruz, J. J., 2003, "Estimating Directional Wave Spectrum Based On Stationary Ship Motion Measurements". Applied Ocean Research, v. 25, pp. 243-261.

[6] Simos, A.N., Sparano, J.V., Tannuri, E. A., Matos, V. L. F., 2009, "Directional Wave Spectrum Estimation Based on a Vessel 1st Order Motions: Field Results". International Journal of Offshore and Polar Engineering, v. 19, pp. 81-89.

[7] Tannuri, E. A. ; Simos, A.N. ; Sparano, J.V. ; Matos, V. L. F. . "Motion-based wave estimation: Small-scale tests with a crane-barge model", Marine Structures, v. 28, p. 67-85, 2012.

[8] Bispo, I. B. S., Simos, A. N., Tannuri, E. A. and Da Cruz, J. J., 2012. "Motion-based wave estimation by a Bayesian inference method: a procedure for pre-defining the hyperparameters". Proceedings of 22nd International Offshore and Polar Engineering Conference, 2012.

[9] Nielsen, U.D., 2005, "Estimation of directional wave spectra from measured ship responses", Ph.D. thesis. Section of Coastal, Maritime and Structural Engineering, Department of Mechanical Engineering, Technical University of Denmark.

[10] Hanson, J.L., and Phillips, O.M., "Automated Analysis of Ocean Surface Directional Wave Spectra", Journal of Atmospheric and Oceanic Technology, 18 February, 2001, pp. 277-293.

[11] Tannuri, E. A., Bispo, I. B. S., Simos, A. N., Queiroz Filho, A. N., da Cruz, J. J. and Carvalho, R. C. A., 2013. "Development of an on-board wave estimation system based on the motions of a moored FPSO: Preliminary assessments from a field campaign.", 32nd International Conference on Ocean, Offshore and Arctic Engineering, OMAE2013, Nantes, France.

[12] Simos, A. N., Tannuri, E. A., Da Cruz, J. J., Queiroz Filho, A. N, Bispo, I. B. S., 2012, Carvalho, R C. A. " Development of an On-Board Wave Estimation System Based on the Motions of a Moored FPSO: Commissioning and Preliminary Validation.", 31th International Conference on Ocean, Offshore and Arctic Engineering, OMAE2012, Rio de Janeiro, Brazil.

[13] Akaike, H., 1980. "Likelihood and Bayes procedure". In Bernardo, J.M., De Groot, M.H., Lindley, D.U. and Smith, A. F.M., Bayesian statistics. Valencia: University Press. pp. 143-166.

[14] Metocean Data – Campos Basin, Technical Specification ET-3000.00-1000-941-PPC-001, rev. B, (2005), Petrobras. (Restricted).